

This article is published as part of the *Dalton Transactions* themed issue entitled:

Self-Assembly in Inorganic Chemistry

Guest Editors Paul Kruger and Thorri Gunnlaugsson

Published in issue 45, 2011 of *Dalton Transactions*

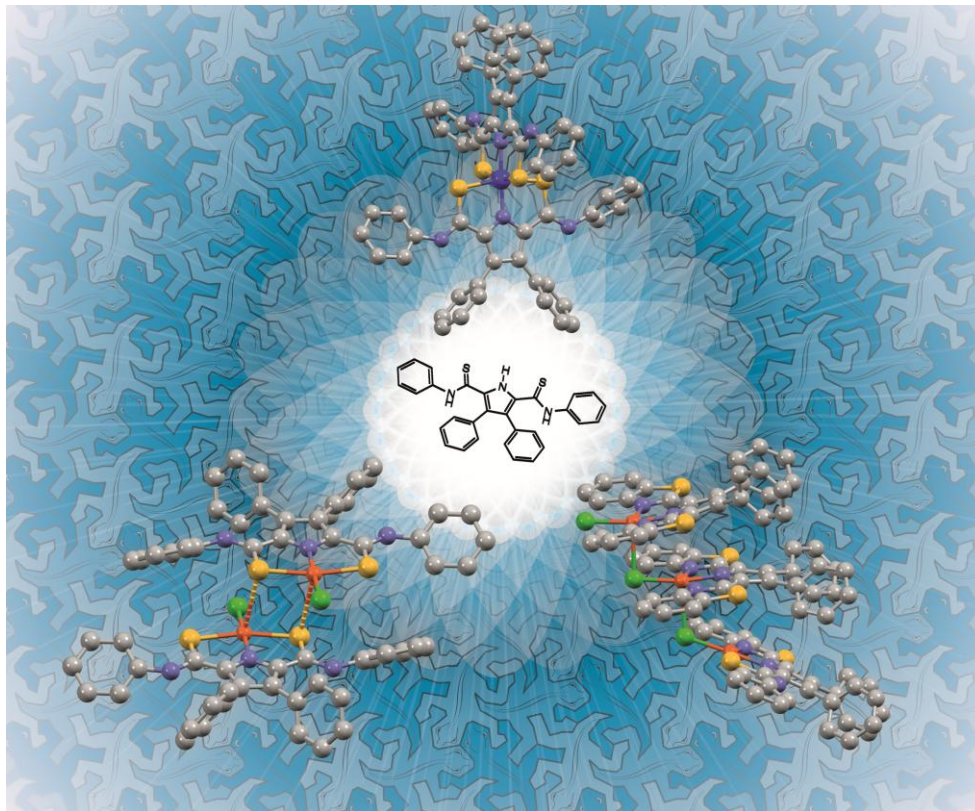


Image reproduced with permission of Mark Ogden

Articles in the issue include:

PERSPECTIVE:

[Metal ion directed self-assembly of sensors for ions, molecules and biomolecules](#)

Jim A. Thomas

Dalton Trans., 2011, DOI: 10.1039/C1DT10876J

ARTICLES:

[Self-assembly between dicarboxylate ions and a binuclear europium complex: formation of stable adducts and heterometallic lanthanide complexes](#)

James A. Tilney, Thomas Just Sørensen, Benjamin P. Burton-Pye and Stephen Faulkner

Dalton Trans., 2011, DOI: 10.1039/C1DT11103E

[Structural and metallo selectivity in the assembly of \[2 × 2\] grid-type metallosupramolecular species: Mechanisms and kinetic control](#)

Artur R. Stefankiewicz, Jack Harrowfield, Augustin Madalan, Kari Rissanen, Alexandre N. Sobolev and Jean-Marie Lehn

Dalton Trans., 2011, DOI: 10.1039/C1DT11226K

Visit the *Dalton Transactions* website for more cutting-edge inorganic and organometallic research

www.rsc.org/dalton

Cite this: *Dalton Trans.*, 2011, **40**, 12235

www.rsc.org/dalton

PAPER

Anion-driven conformation control and enhanced sulfate binding utilising aryl linked salicylaldoxime dicopper helicates†

James R. Stevens and Paul G. Plieger*

Received 1st May 2011, Accepted 26th July 2011

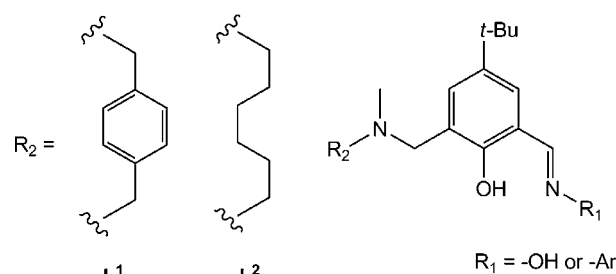
DOI: 10.1039/c1dt10808e

The synthesis and spectroscopic analysis of both “metal-only” and anion encapsulated dicopper(II) double helicates utilising a new 1,4-aryl spacer is described. X-Ray crystallographic analysis of the complexes reveal that the aromatic spacer increases rigidity in the complex, yet the complexes are still able to undergo a dramatic “coiling up” to bind anions. Spectroscopic analysis has shown a clear enhancement in the binding strength of SO_4^{2-} over the non-coordinating anions ClO_4^- , NO_3^- and Br^- which has been attributed to a combination of enhanced rigidity in the complex and an increased electrostatic interaction between the complex and the dianion.

Introduction

The binding and extraction of anions continues to receive intense attention due to the great importance these molecules play in a variety of environmental, biological and commercial applications.¹ Ditopic receptors designed for simultaneous binding of both cations and their attendant anions is a challenging task due to the specific requirements needed to be met by both the metal coordinating site and the anion binding site/pocket.² Nevertheless there continues to be innovative and well designed examples reported on a regular basis.³

In the last few years we have devoted some time to exploring anion binding complexes that have been designed to specifically encapsulate anions within dicopper helicates. These complexes contain metal complexation sites utilising salicylaldimine^{4,5} or salicylaldoxime^{6,7} units which are linked to one another *via* spacers of alkyl tertiary amines (L^2 in Scheme 1). Upon complexation the complexes self assemble and form neutral di-metallic helicates. When these groups of anion receptors are further protonated, they are able to exist in a zwitterionic state and form both hydrogen bonds and (in some cases) metal covalent bonds with encapsulated anions.^{4–7} We have shown that dramatic conformational changes can occur within these complexes upon binding an anion; the complexes coil up and there is a substantial contraction of the central cavity within the complex, bringing the Cu(II) centres closer together with a corresponding increase in the helix twist angle of the complex. Anion binding studies with this complex however showed only minor changes in anion binding *strength* in non-aqueous media⁶ yet were shown to be *selective* for both sulfate and



Scheme 1 General form of the ligands used to make the dicopper helicates.

dihydrogen phosphate in aqueous media.⁷ Further, deprotonation of the oxime groups can lead to extended hexanuclear trihelicates.⁸

In this paper, we demonstrate that a decrease in ligand conformational flexibility can lead to an enhancement in anion binding strength. This has been achieved by the substitution of a six-carbon alkyl spacer (L^2 Scheme 1) which is used to link two salicylaldoxime units together with that of a six carbon *aromatic* spacer (L^1 Scheme 1). This minor change has led to a clear enhancement in the binding strength of sulfate over other non-coordinating anions.

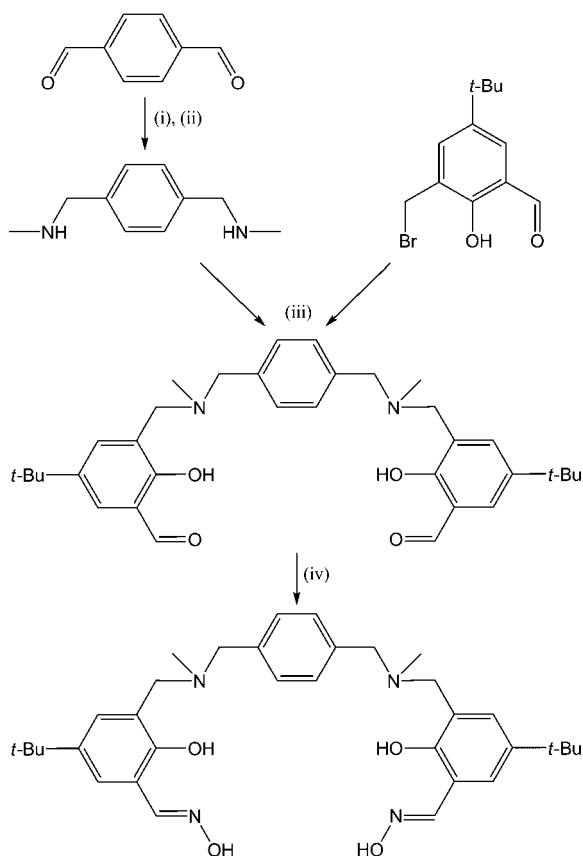
Results and discussion

Synthesis of the ligands

Ligand L^1 was prepared from terephthalaldehyde as outlined in Scheme 2. Condensation of the resulting secondary diamines with 3-(bromomethyl)-5-*tert*-butyl-2-hydroxybenzaldehyde⁹ in dichloromethane resulted in the formation of the aromatic linked salicylaldehyde. Subsequent oximation gave the final ligand in an overall yield of 43%. The ligand was fully characterised including X-ray structural analysis (see experimental and ESI†).

Institute of Fundamental Sciences, Massey University, Private Bag 11 222, Palmerston North, New Zealand. E-mail: p.g.plieger@massey.ac.nz; Fax: 0064 6 350 5682; Tel: 0064 6 356 9099, extension 7825

† Electronic supplementary information (ESI) available: X-Ray of the ligand L^1 and further descriptions of the structures of **3** and **4**. CCDC reference numbers 824379–824382. For ESI and crystallographic data in CIF or other electronic format, see DOI: 10.1039/c1dt10808e



Scheme 2 Ligand synthesis of L^1 . Reagents and conditions: (i) $\text{MeNH}_2 \cdot \text{HCl}/\text{KOH}$, MeOH , rt, 2 h; (ii) $\text{NaBH}_4/\text{MeOH}$, rt, 1 h; (iii) Et_3N , CH_2Cl_2 , rt, 15 h; (iv) $\text{NH}_2\text{OH} \cdot \text{HCl}/\text{KOH}$, EtOH , rt, 15 h.

Formation of “metal only” complexes

The anion-free charge-neutral dinuclear $\text{Cu}(\text{II})$ complex $[\text{Cu}_2(\text{L}^1\text{-}2\text{H})_2]$ (**1**), was readily isolated from the reaction of the ligands with copper acetate in a manner akin to that used to prepare complexes of L^2 previously.⁶ Microanalysis, ESMS and X-ray structure determination (see below) all confirmed the general formula of the complex. The complex consists of two $\text{Cu}(\text{II})$ atoms coordinated to two ligand molecules with each copper centre sharing both ligands *via* coordination to the N-oximate and phenolate positions ($\text{N}_2\text{O}_2^{2-}$). Head-to-tail hydrogen-bonding of the salicylaldoxime ligand dominate the coordination site providing a near square planar coordination geometry for $\text{Cu}1$ and a square pyramidal geometry for $\text{Cu}2$ which possess a weak fifth phenolate oxygen donor from an adjacent complex (Fig. 1 and Table 1). In **1** each 1,4-aryl linker (one from each ligand) is wound around one another in a helical fashion with each salicylaldoxime ring sitting above a corresponding ring from the opposing ligand and the aryl groups in the spacers sit edge-on to one another. There is a CHCl_3 molecule encapsulated within the complex making a weak H-bond to π interaction to one of the phenolate rings of $3.50(1)$ Å. The rigid nature of the spacer has resulted in a copper–copper distance for **1** of $8.2588(9)$ Å and a helix twist angle of $78.7(2)^\circ$ (the mean of the two $\text{O}-\text{Cu}-\text{Cu}-\text{O}$ angles), which is considerably shorter and less twisted than the corresponding distance and angle for the more floppy complex $[\text{Cu}_2(\text{L}^2\text{-}2\text{H})_2]$ at $10.191(3)$ Å and $85.9(3)^\circ$ respectively.⁶

Table 1 Selected bond lengths and angles for the $\text{Cu}(\text{II})$ centres of **1**

Atoms	Bond lengths (Å)	X–Cu–X	Bond angles ($^\circ$)
$\text{Cu}1-\text{O}11$	1.852(2)	$\text{O}11-\text{Cu}1-\text{N}212$	93.5(1)
$\text{Cu}1-\text{O}12$	1.870(2)	$\text{O}11-\text{Cu}1-\text{N}222$	87.3(1)
$\text{Cu}1-\text{N}212$	1.950(1)	$\text{O}12-\text{Cu}1-\text{N}212$	88.6(1)
$\text{Cu}1-\text{N}222$	1.947(1)	$\text{O}12-\text{Cu}1-\text{N}222$	92.6(1)
$\text{Cu}2-\text{O}13$	1.865(1)	$\text{O}13-\text{Cu}2-\text{N}232$	92.6(1)
$\text{Cu}2-\text{O}14$	1.863(1)	$\text{O}13-\text{Cu}2-\text{N}242$	87.8(1)
$\text{Cu}2-\text{N}232$	1.946(2)	$\text{O}14-\text{Cu}2-\text{N}232$	89.3(1)
$\text{Cu}2-\text{N}242$	1.953(2)	$\text{O}14-\text{Cu}2-\text{N}242$	92.6(1)
$\text{Cu}2-\text{O}12b$	2.9109(1)	$\text{O}13-\text{Cu}2-\text{O}12b$	86.9(1)
$\text{Cu}1-\text{Cu}2$	8.2588(9)	$\text{O}11-\text{Cu}1-\text{Cu}2-\text{O}13$	78.3(1)
		$\text{O}12-\text{Cu}1-\text{Cu}2-\text{O}14$	79.2(1)

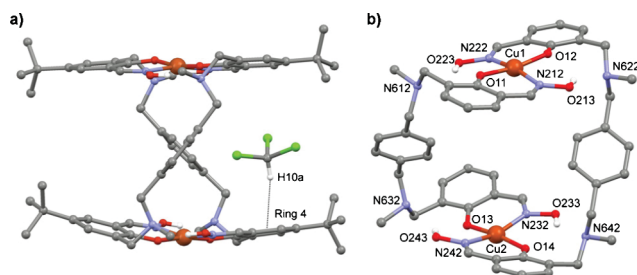


Fig. 1 Perspective views of **1** showing the edge on nature of the aryl linkers and positioning of the CHCl_3 solvent molecule (a) and copper coordination site with labels (b). Hydrogen atoms not involved in H-bonding have been omitted for clarity.

Formation of metal salt complexes

Examples of $\text{Cu}(\text{II})$ salt complexes containing the anions ClO_4^- , NO_3^- , SO_4^{2-} , BF_4^- , and Br^- were readily prepared by direct combination of L^1 and the appropriate $\text{Cu}(\text{II})$ salt in methanol. Crystals suitable for X-ray structure determination were obtained for $[\text{ClO}_4\text{C}u_2\text{L}^1_2](\text{ClO}_4)_3$ (**3**) (Fig. 2) and $[\text{BF}_4\text{C}u_2\text{L}^1_2](\text{BF}_4)_3$ (**4**) to determine the extent to which a restrictive spacer might influence both anion binding and cavity geometries. Comparisons have also been made with metal salt complexes of L^2 which have been communicated previously.^{6,7}

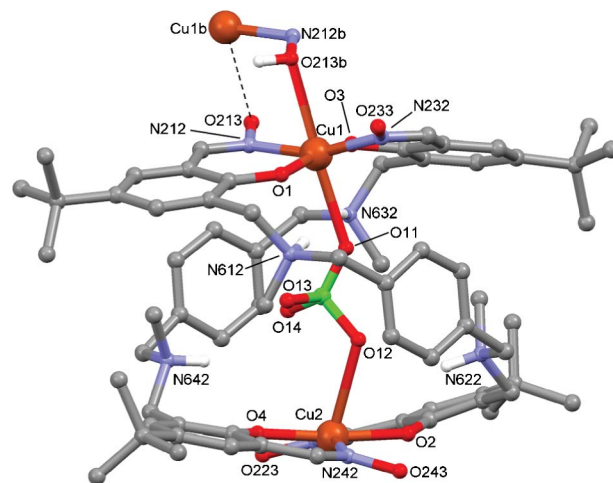


Fig. 2 Perspective view of $[\text{ClO}_4\text{C}u_2\text{L}^1_2]^+$, showing the atom labelling scheme and the weakly coordinated axial $\text{O}-\text{N}-\text{Cu}$ atoms of an adjacent complex. Hydrogen atoms, disorder around the central perchlorate (50 : 50) and the three counter perchlorate anions have been omitted for clarity.

Table 2 Selected bond lengths and angles at the Cu(II) centres of **3**

Atoms	Bond lengths (Å)	X–Cu–X	Bond angles (°)
Cu1–O1	1.900(4)	O1–Cu1–N212	92.7(2)
Cu1–O3	1.907(4)	O1–Cu1–N232	90.8(2)
Cu1–N212	1.942(6)	O3–Cu1–N212	87.4(2)
Cu1–N232	1.952(6)	O3–Cu1–N232	91.7(2)
Cu1–O11	2.487(11)	O11–Cu1–O1	89.9(4)
Cu1–O213b	2.853(3)	O213b–Cu1–O1	84.5(2)
Cu2–O2	1.931(5)	O2–Cu2–N222	91.6(2)
Cu2–O4	1.907(4)	O2–Cu2–N242	89.6(2)
Cu2–N222	1.953(6)	O4–Cu2–N222	88.4(2)
Cu2–N242	1.933(6)	O4–Cu2–N242	91.9(2)
Cu2–O12	2.606(11)	O12–Cu2–O2	76.5(3)
		O1–Cu1–Cu2–O2	129.8(2)
Cu1–Cu2	7.135(2)	O3–Cu1–Cu2–O4	128.3(2)

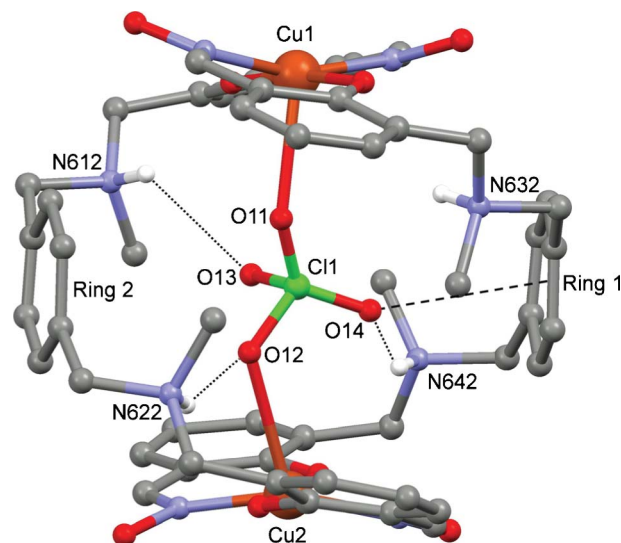
The coordination environment for each copper atom in **3** is similar to **1** above with both Cu(II) atoms coordinated to two L^1 ligands through N-oximate and phenolate donors ($N_2O_2^{2-}$). Both copper atoms coordinate to oxygen atoms of the encapsulated perchlorate anion and Cu1 has an additional weak interaction to an oximate O atom on an adjacent complex situated directly above it. The coordination environments for Cu1 and Cu2 are therefore best described as distorted octahedral and distorted square pyramidal respectively (see Table 2 for selected bond lengths and angles around the metal centres). The pseudo macrocyclic cavity surrounding each metal centre is completed by an oxime hydrogen bonded towards the opposing phenolate oxygen with an average distance of ~ 2.72 Å which is buttressed with a secondary H-bond from each protonated tertiary amine on the spacer to the phenolate oxygen atoms with an average distance of ~ 2.90 Å (refer to Table 3 for H-bond distances and angles). Each tertiary amine in the aryl containing spacer of L^1 is protonated and located around the periphery are three perchlorate anions giving rise to an overall neutral complex.

Located at the centre of the complex, flanked by both the metal centres and the aryl rings of the spacer, is a ClO_4^- anion. It sits comfortably inside the cavity created by the complex and the complex has contracted significantly in the process so that both of the copper(II) centres are able to make weak interactions with this traditionally non-coordinating anion. This encapsulated anion is stabilised by three distinct interactions; there are two Cu–O bonds

Table 3 Selected H-bond and anion– π distances and angles for **3**

Atoms	D–H–A distance (Å)	D–H–A angle (°)
N622–H62j...O12	3.08(1)	143.6
N612–H61j...O13	2.99(2)	115.9
N642–H64j...O14	3.30(2)	147.7
N632–H63j...O11A	2.84(2)	145.4
N612–H61j...O13A	3.29(2)	135.0
N642–H64j...O14A	2.95(1)	128.6
O213–H213...O3	2.63(1)	132.8
O223–H223...O4	2.66(1)	132.4
O233–H233...O1	2.85(1)	125.8
O243–H243...O2	2.73(1)	130.7
N612–H61j...O1	2.81(1)	130.0
N622–H62j...O2	2.88(1)	128.0
N632–H63j...O3	2.94(1)	126.0
N642–H64j...O4	2.96(1)	124.0
Cl1–O14...Ring 1	3.02	151.9
Cl1–O13a...Ring 2	3.04	157.8

of similar distance (Cu1–O11 2.4857(3) and Cu2–O12 2.6062(2) Å) between two of the oxygen atoms from the central anion and each copper atom. Secondly, there exists three moderate to weak hydrogen bonds (range = 2.839–3.295 Å for $N \cdots F$ distances) for each disordered orientation of the anion, originating from the four protonated tertiary amines on the two spacers which all point inwards towards the central cavity (see Fig. 3 and Table 3 for hydrogen bond distances and angles). Finally, in contrast to the “metal-only” complex **1**, the aryl groups are now rotated so the aryl rings face towards the anion forming an anion– π interaction^{10,11} at a distance of 3.02 and 3.04 Å for each of the positionally disordered sites of the anion. These two anion– π distances are relatively strong compared to other perchlorate oxygen– π interactions of this type, possibly as a consequence of the restricted movement this anion possesses within the cavity.¹⁰

**Fig. 3** Perspective view of $[ClO_4^- \subset Cu_2L_2]^{3+}$ showing one disordered position of the ClO_4^- anion and both the H-bonding of the anion to the ammonium groups and the anion– π interaction to the aryl ring of the linker. Hydrogen atoms not involved in hydrogen bonding, the *tert*-butyl groups and counter anions have been omitted for clarity.

The distance between the two copper(II) centres in **3** has reduced markedly from 8.2588(9) to 7.135(2) Å ($\Delta \approx 1.12$ Å or 14%) upon encapsulating the perchlorate anion, in addition, the average helix twist angle (O–Cu–Cu–O) of **3** has increased substantially by over 50° to $129.0(4)^\circ$. This indicates that this more rigid aromatic spacer still imparts sufficient flexibility to allow the complex to coil up to accommodate the encapsulated ClO_4^- anion. The coordination geometry around the copper metals has been influenced slightly with the incorporation of the anion. The average Cu–O bond distance has increased slightly (0.05 Å) and the average O–Cu–O bond angle is now slightly more linear (173.5°). Conversely, the Cu–N bond distance has remained unchanged and the average N–Cu–N bond angle is now more bent (161.6°). The weak intermolecular bond to the copper seen in **1** is retained in **3**.

The overall structural features of **4** are similar to **3**. Both Cu(II) centres in **4** have the same *trans* arrangement as the four in-plane donors of **3**. The pseudo macrocyclic cavity surrounding each metal centre is retained with oxime to phenolate hydrogen bonds again buttressed with secondary H-bonds to each

Table 4 Selected bond lengths and angles for **4**

Atoms	Bond lengths (Å)	X–Cu–X	Bond angles (°)
Cu1–O11	1.881(4)	O11–Cu1–N212	92.1(2)
Cu1–O14	1.903(4)	O11–Cu1–N242	89.1(2)
Cu1–N212	1.955(5)	O14–Cu1–N212	88.9(2)
Cu1–N242	1.952(5)	O14–Cu1–N242	91.2(2)
Cu2–O13	1.894(3)	O12–Cu2–N222	92.3(2)
Cu2–O12	1.896(3)	O12–Cu2–N232	89.7(2)
Cu2–N222	1.951(4)	O13–Cu2–N222	88.0(2)
Cu2–N232	1.932(5)	O13–Cu2–N232	92.1(2)
Cu2–F11b	2.538(2)	F11b–Cu2–O12	76.5(4)
Cu1–Cu2	7.212(1)	O11–Cu1–Cu2–O12	130.7(2)
F11...Cu2	2.84(2)	O14–Cu1–Cu2–O13	130.4(2)
F11b...Cu2	2.54(1)	O12–Cu2–F11	74.3(4)
F14...Cu1	2.63(1)	O12–Cu2–F11b	76.4(3)
F14b...Cu1	3.10(1)	O14–Cu1–F14	73.2(3)
		O14–Cu1–F14b	69.2(2)
Atoms	Bond lengths (Å)	Atoms	Bond lengths (Å)
O213...O14	2.693(5)	N612...O11	2.981(6)
O223...O13	2.649(5)	N622...O12	2.818(5)
O233...O12	2.756(5)	N632...O13	3.003(5)
O243...O11	2.707(5)	N642...O14	2.877(6)

phenolate oxygen from the protonated tertiary amines. The occluded tetrafluoroborate anion is positionally disordered over two sites in a 60:40 ratio. Each disordered position has one weak bonding interaction between one fluorine atom and one of the copper atoms but in opposing directions, therefore, the coordination environments for the Cu(II) centres in **4** are described as distorted square planar (Cu1) and distorted square pyramidal (Cu2) for the major component of the disorder and the reverse description for the minor component (refer to Table 4 for selected bond distances and angles).

The distance between the two Cu(II) centres in **4** at 7.212(1) Å has decreased significantly from that of **1**, but is only slightly larger than that of **3**. The average helical twist angle has again increased significantly over **1** but is comparable to **3** at 130.6°. Therefore it appears that while the complex has again coiled up to accommodate this anion it may now have reached its limit of conformational flexibility and may not be able to further contract for this slightly smaller anion. An inspection of the H-bonds around the entrapped BF₄[−] anion reveals hydrogen bonding now plays a more dominant role in stabilising the anion with each disordered tetrafluoroborate now stabilised by four moderate hydrogen bonds.

Similarly to **3**, the anion–π interaction is again present but is weaker at distances of 3.31 and 3.10 Å, for the major and minor components of the disordered BF₄[−] anion respectively (Fig. 4 and Table 5). Overall there appears to be a subtle shift away from stabilisation utilising metal–anion bonds towards an increased role in stabilisation by hydrogen bonding as a consequence of both reduced anion volume and restrictive conformational flexibility of the receptor.

Anion binding studies

The “copper only” complex was subjected to UV-Vis titration experiments in THF to quantify the effect that a more rigid spacer has with regards to anion affinity. Preliminary stability constants have been calculated for SO₄^{2−}, NO₃[−], ClO₄[−] and Br[−] anions and are shown in Table 6.

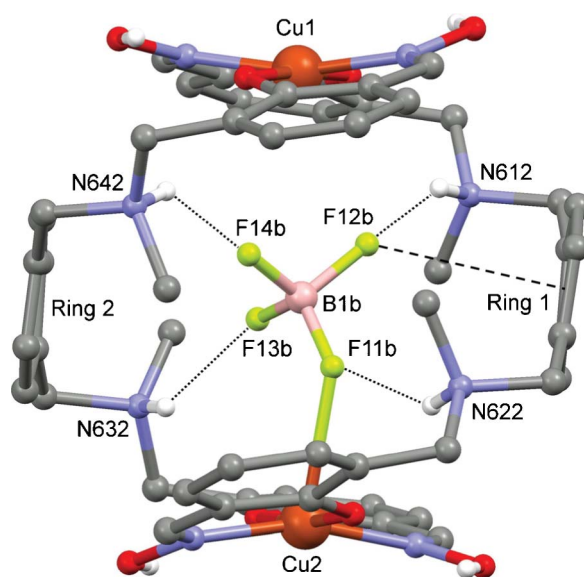


Fig. 4 Perspective view of [BF₄–Cu₂L₂]³⁺ showing the major component (60%) of the disordered BF₄[−] with H-bonding to the ammonium groups and the anion–π interaction to the aryl ring on the spacer. Hydrogen atoms not involved in hydrogen bonding, the *tert*-butyl groups, the minor component of the anion disorder (40%) and the peripheral counter anions have been omitted for clarity.

Table 5 Selected H-bond distances, angles and anion–π interactions between the encapsulated BF₄[−] anion and the complex **4**

Atoms	H-bond distances (Å)	D–H–A angles (°)
N622–H62j...F11	3.01(2)	137.7
N612–H61j...F12	2.92(1)	126.3
N632–H63j...F13	3.00(1)	150.2
N642–H64j...F14	3.12(1)	146.0
N622–H62j...F11b	3.17(1)	144.1
N612–H61j...F12b	3.08(1)	149.8
N632–H63j...F13b	2.92(1)	131.2
N642–H64j...F14b	2.81(1)	135.0
B1–F13...Ring 2	3.10	133.5
B1b–F12b...Ring 1	3.31	124.0

Table 6 Formation constants of [X^{n−}–Cu₂L₂]^{(4−n)+} obtained from spectrophotometric titrations^a of **1** with H₂SO₄, HClO₄, HBr, and HNO₃ in THF at 294 K

Acid/anion	log K
H ₂ SO ₄	5.53 ± 0.32
HClO ₄	3.86 ± 0.22
HNO ₃	3.72 ± 0.08
HBr	3.69 ± 0.17

^a For the reaction [Cu₂L₂]⁴⁺ + X^{n−} ⇌ [X^{n−}–Cu₂L₂]^{(4−n)+} involving complexes with L¹ in its zwitterionic form with both aminomethyl substituents protonated.

The binding constants given in Table 4 vary in the order Br[−] ≈ NO₃[−] ≈ ClO₄[−] ≪ SO₄^{2−}. This order is consistent with the stability of the [X^{n−}–Cu₂L₂]^{(4−n)+} complexes being dependent on a combination of anion charge, size, shape, coordination ability to the copper atoms and ability to form hydrogen bonds to the N–H in the alkylammonium groups. These factors favour the inclusion of the dianion sulfate, yet there appears to be an added enhancement

in binding strength towards sulfate for the more conformationally restricted **L**¹ (+1.7 log units) when the data is compared against that for the **L**² inclusion complexes (−0.1 log units).⁶ For the weakly coordinating anions, ClO₄[−], NO₃[−] and Br[−] there appears to be no discernible difference in binding strength. The inclusion of the aryl ring in the spacer may have reduced the dependency on anion shape for the binding of these anions.

Conclusion

The inclusion of aromatic spacers in the salicylaldehyde ligand spacers of these complexes has led to a number of changes in the anion binding characteristics of complexes of this type. The increase in rigidity has played a major role in the clear enhancement in strength of binding sulfate over the non-coordinating anions. Less of an effect, if at all any, has been noticed with the introduction of groups capable of anion– π interactions. In fact, the addition of these aromatic spacers appears to minimise differences in binding strength attributed to the shape of the anions. Work continues with us to further probe this theory.

Experimental

Unless specified, commercial reagents and solvents were used without purification. ¹H and ¹³C NMR spectra were recorded on Bruker Avance 400 MHz and 500 MHz spectrometers; δ values are relative to TMS or the corresponding solvent. Mass spectra were obtained using a Micromass ZMD 400 electrospray spectrometer. IR spectra were recorded on a Nicolet 5700 FT-IR spectrometer from Thermo Electron Corporation using an ATR sampling accessory. UV-Vis spectra were recorded in THF using a CARY 100Bio UV-Vis spectrometer. Elemental analyses were determined by the Campbell Microanalytical Laboratory at the University of Otago.

Synthesis of ligands

***N,N'*-Dimethyl-*p*-xylylenediamine (1a).** A solution of methylamine hydrochloride (3.115 g, 46.1 mmol) in methanol (60 ml) was allowed to mix with a solution of potassium hydroxide (2.788 g, 49.7 mmol) in methanol (60 ml). The filtered solution was slowly dripped into a second solution of terephthalaldehyde (2.106 g, 15.7 mmol) in methanol (80 ml) over 1 h. The pale yellow solution was stirred at rt for 2 h. Sodium borohydride (1.256 g, 33.2 mmol) was added portion wise to the stirred solution over 10 min, which was then left to stir for 1 h. The solvent was removed under reduced pressure and the resulting white solid was dissolved in chloroform (70 ml) and washed with water (50 ml). The organic layer was separated and dried over anhydrous MgSO₄. The solvent was removed under reduced pressure, leaving a pale yellow oil, which upon standing, solidified into a white solid (2.128 g, 83%). δ_{H} (500 MHz; CDCl₃; Me₄Si): 7.27 (4H, s, ArH), 3.73 (4H, s, CH₂), 2.45 (6H, s, CH₃), 1.33 (2H, br s, NH). δ_{C} (125 MHz; CDCl₃; Me₄Si): 139.1 (ArCHArCH), 128.4 (ArCH), 56.0 (CH₂), 36.2 (CH₃). m/z (ESI) 165.45 (**1a**)⁺. ν_{max} /cm^{−1} 3259br (N–H), 810s (Ar–H).

3,3'-(1,4-Phenylenebis(methylene))bis(methylazanediy)bis(methylene)bis(5-*tert*-butyl-2-hydroxybenzaldehyde) (1b). To a stirred solution of triethylamine (1.316 g, 13.0 mmol) in

dichloromethane (50 ml) were added simultaneously and slowly (over 1 h) solutions of 3-(bromomethyl)-5-*tert*-butyl-2-hydroxybenzaldehyde (3.345 g, 12.3 mmol) in dichloromethane (50 ml) and *N,N'*-dimethyl-*p*-xylylenediamine (1.013 g, 6.5 mmol) in methanol/dichloromethane (1:20, 50 ml). The resulting mixture was left to stir at rt overnight. The reaction was monitored for completion *via* ¹H-NMR. The solvent was evaporated to dryness and the yellow solid was redissolved in chloroform (80 ml) then filtered. The organic layer was washed with water (3 × 30 ml), separated and dried over anhydrous MgSO₄. The solvent was removed under reduced pressure and dried *in vacuo* to give a bright yellow solid (3.262 g, 97%). δ_{H} (500 MHz; CDCl₃; Me₄Si): 10.32 (2H, s, CHO), 7.62 (2H, d, $J = 2.3$ Hz, ArH), 7.38 (2H, d, $J = 1.8$ Hz, ArH), 7.31 (4H, s, ArH), 3.74 (4H, s, CH₂), 3.61 (4H, s, CH₂), 2.26 (6H, s, NCH₃), 1.28 (18H, s, C(CH₃)₃). δ_{C} (125 MHz; CDCl₃; Me₄Si): 192.4 (CHO), 159.3 (COH), 142.1 (ArC), 136.7 (ArC), 133.1 (ArCH), 129.6 (ArCH), 125.1 (ArCH), 124.0 (ArC), 122.1 (ArC), 61.5 (CH₂), 59.1 (CH₂), 41.8 (NCH₃), 34.3 (C(CH₃)₃), 31.5 (C(CH₃)₃). Found: C, 74.21; H, 8.31; N, 4.78%. C₃₄H₄₄N₂O₄·0.3H₂O requires C, 74.23; H, 8.17; N, 5.09%. m/z (ESI) 545.71 (**1b**)⁺. ν_{max} /cm^{−1} 2962br (C–H), 1676s (C=O), 1216s (C–O), 825s (Ar–H). Mp 129.2–131.1 °C.

(1E,1'E)-5-*tert*-Butyl-3-(((4-(((5-*tert*-butyl-2-hydroxy-3-((E)-hydroxyimino)methyl)benzyl)(methylamino)methyl)benzyl)-(methylamino)methyl)-2-hydroxybenzaldehyde oxime (L¹). A solution of hydroxylamine hydrochloride (0.400 g, 5.76 mmol) in ethanol (60 ml) was added to a solution of potassium hydroxide (0.324 g, 5.77 mmol) in ethanol (60 ml). The resulting white precipitate was removed by filtration. The filtered solution was slowly dripped into a solution of **1b** (1.032 g, 1.90 mmol) in a chloroform/ethanol mix (1:20, 100 ml) over 2 h. The pale yellow solution was then allowed to stir at rt overnight. The solution was removed under reduced pressure, dissolved in chloroform (50 ml) and washed with water (2 × 20 ml). The organic layer was separated and dried over anhydrous MgSO₄, filtered and dried to give a pale yellow solid. The product could be further purified by crystallisation from hot toluene to give colourless block shaped crystals (0.580 g, 53%). δ_{H} (400 MHz; CDCl₃; Me₄Si): 10.09 (2H, br s, NOH), 8.46 (2H, s, CHNOH), 7.44 (2H, d, $J = 2.1$ Hz, ArH), 7.32 (4H, s, ArH), 7.15 (2H, d, $J = 2.1$ Hz, ArH), 3.75 (4H, s, CH₂), 3.63 (4H, s, CH₂), 2.27 (6H, s, NCH₃), 1.30 (18H, s, C(CH₃)₃). δ_{C} (100 MHz; CDCl₃; Me₄Si): 154.3 (COH), 148.7 (CHNOH), 141.8 (ArC), 136.3 (ArC), 129.7 (ArCH), 128.2 (ArCH), 123.9 (ArCH), 122.5 (ArC), 117.7 (ArC), 61.2 (CH₂), 59.3 (CH₂), 41.6 (NCH₃), 34.1 (C(CH₃)₃), 31.5 (C(CH₃)₃). Found: C, 72.21; H, 8.11; N, 9.22%. C₃₄H₄₆N₄O₄·0.5C₇H₈ requires C, 72.55; H, 8.12; N, 9.02%. m/z (ESI) 575.85 (**L**¹)⁺. ν_{max} /cm^{−1} 2955br (C–H), 1615m (C=N), 1268s (C–O), 824s (Ar–H). Mp 126 °C.

General Cu(II) complex synthesis with L¹

To a stirred pale yellow solution of **L**¹ (9.00 mmol L^{−1}) in methanol/chloroform (10:1) was slowly added dropwise 1 mole equivalent of the copper(II) salt (12.00 mmol L^{−1}) in methanol over 30 min. The resulting coloured solution was stirred for 20 h. The solvent was evaporated to dryness. The crude product was then purified by recrystallisation.

“Copper only” complex, [Cu₂(L¹-2H)₂] (1). The general method outlined above was followed using copper(II) acetate monohydrate. The crude brown product was purified by recrystallisation with diisopropyl ether diffusion from chloroform to afford brown platelet crystals. The crystals were collected and washed with diisopropyl ether (0.1134 g, 15%). Found: C, 56.49; H, 6.38; N, 7.05%. C₆₈H₈₈N₈O₈Cu₂·2CHCl₃·0.5DIPE requires C, 56.12; H, 6.26; N, 7.17%. *m/z* (ESI) 636.79 [(L¹-H)Cu]⁺. UV-Vis (THF, 1.5 × 10⁻⁵ mol L⁻¹) λ_{max}/nm (ε/L mol⁻¹ cm⁻¹): 350 (21 000), 273 (60 700), 256 (72 800). ν_{max}/cm⁻¹ 3137brw (O–H), 1625m (C=N), 1216s (C–O), 836s (Ar–H).

[SO₄⊂(Cu₂L₂)](SO₄)₃ (2). The general method outlined above was followed using copper(II) sulfate pentahydrate. The dark green product was purified by recrystallisation with diisopropyl ether diffusion from methanol. The green precipitate was collected and washed with diisopropyl ether (0.040 g, 26%). Found: C, 48.68; H, 6.28; N, 6.42%. C₆₈H₉₂N₈O₂₄S₄Cu₂·2.5 MeOH requires C, 48.64; H, 5.91; N, 6.44%; *m/z* (ESI) 734.38 [(SO₄L¹Cu)]⁺. UV-Vis (THF/0.1% MeOH, 2.0 × 10⁻⁵ mol L⁻¹) λ_{max}/nm (ε/L mol⁻¹ cm⁻¹): 310 (15 900); ν_{max}/cm⁻¹ 1630brm (C=N), 1101brs (SO₄), 838w (Ar–H).

[ClO₄⊂(Cu₂L₂)](ClO₄)₃ (3). The general method outlined above was followed using copper(II) perchlorate hexahydrate. The green/grey product was purified by recrystallisation with diisopropyl ether diffusion from acetonitrile to afford green chunky crystals. The crystals were collected and washed with diisopropyl ether (0.147 g, 50%). Found: C, 47.43; H, 5.61; N, 6.49%. C₆₈H₉₂N₈O₂₄Cl₄Cu₂·3H₂O requires C, 47.25; H, 5.71; N, 6.48%; *m/z* (ESI) 736.67 [(ClO₄L¹Cu)]⁺. UV-Vis (THF/0.5% MeCN, 2.0 × 10⁻⁵ mol L⁻¹) λ_{max}/nm (ε/L mol⁻¹ cm⁻¹): 351 (8600), 270 (26 200); ν_{max}/cm⁻¹ 3132brw (O–H), 1631m (C=N), 1091brs (ClO₄), 838w (Ar–H).

[BF₄⊂(Cu₂L₂)](BF₄)₃ (4). The general method outlined above was followed using copper(II) tetrafluoroborate monohydrate. The crude green product was purified by recrystallisation with diethyl ether diffusion from acetone to afford brown platelet crystals. The crystals were collected and washed with diethyl ether (0.034 g, 16%). Found: C, 50.35; H, 5.97; N, 6.64%. C₆₈H₉₂N₈O₈B₄F₁₆Cu₂ requires C, 50.30; H, 5.71; N, 6.90%. *m/z* (ESI) 636.16 [(L¹-H)Cu]⁺; UV-Vis (THF/0.2% MeCN, 2.0 × 10⁻⁵ mol L⁻¹) λ_{max}/nm (ε/L mol⁻¹ cm⁻¹): 351 (17 600), 270 (54 400), 256 (63 000); ν_{max}/cm⁻¹ 1630w (C=N), 1053brs (BF₄), 838w (Ar–H).

[NO₃⊂(Cu₂L₂)](NO₃)₃ (5). The general method outlined above was followed using copper(II) nitrate trihydrate. The dark green product was purified by recrystallisation with diisopropyl ether diffusion from a methanol/acetonitrile (4:1) mix. The dark green precipitate was collected and washed with diisopropyl ether (0.122 g, 37%). Found: C, 52.84; H, 6.46; N, 11.07%. C₆₈H₉₂N₁₂O₂₀Cu₂·H₂O requires C, 52.94; H, 6.14; N, 10.90%; *m/z* (ESI) 699.77 [(NO₃L¹Cu)]⁺, 668.22 [(L¹Cu)₂NO₃]²⁺; UV-Vis (THF/0.5% acetone, 2.0 × 10⁻⁵ mol L⁻¹) λ_{max}/nm (ε/L mol⁻¹ cm⁻¹): 338 (13 500), 289 (60 100), 260 (75 700); ν_{max}/cm⁻¹ 1660s (C=N), 1295brs (NO₃), 839m (Ar–H).

[Br⊂(Cu₂L₂)](Br)₃ (6). The general method outlined above was followed using copper(II) bromide. The dark brown product was purified by recrystallisation with diethyl ether diffusion from

acetonitrile. The dark brown precipitate was collected and washed with diethyl ether (0.082 g, 28%). Found: C, 42.81; H, 4.97; N, 6.10%. C₆₈H₉₂N₈O₈Br₄Cu₂·4HBr requires C, 42.54; H, 5.04; N, 5.84%; *m/z* (ESI) 718.61 [(BrL¹Cu)]⁺; UV-Vis (THF/0.1% MeOH, 2.0 × 10⁻⁵ mol L⁻¹) λ_{max}/nm (ε/L mol⁻¹ cm⁻¹): 670 (825), 386 (7300), 333 (19 300), 311 (23 100); ν_{max}/cm⁻¹ 1621m (C=N), 834s (Ar–H).

X-Ray structure determination

X-Ray data were recorded at low temperature with a Rigaku Spider X-ray diffractometer, comprising a Rigaku MM007 microfocus copper rotating-anode generator, high-flux Osmic monochromating and focusing multilayer mirror optics (Cu K radiation, λ = 1.5418 Å), and a curved image-plate detector. *CrystalClear*¹² was utilized for data collection and *FSPProcess* in *PROCESS-AUTO*¹³ for cell refinement and data reduction. All structures were solved employing direct methods and expanded by Fourier techniques.¹⁴ Non-hydrogen atoms were refined anisotropically. Hydrogen atoms were placed in calculated positions and refined using a riding model with fixed isotropic *U* values. The encapsulated perchlorate anion within **3** and one of the attendant perchlorate anions are both disordered over two sites in a 50:50 ratio. Likewise the encapsulated tetrafluoroborate anion in **4** is also disordered (60:40). There exists rotational disorder on a number of *tert*-butyl groups in **4** (50:50). Disordered solvent regions in the structures **1**·CHCl₃ and **3** were treated in the manner described by van der Sluis and Spek,¹⁵ resulting in the removal of 47 and 258 e⁻ per cell respectively. These values approximate to C₆H₁₄O (58) and 2C₆H₁₄O + 0.5CH₃CN (127) per formula unit respectively.

Crystal data for [Cu₂(L¹-2H)₂]·CHCl₃ (1)·CHCl₃. 2(C₆₈H₈₄Cu₂N₈O₈), 0.5(C₂H₂Cl₆) *M_r* = 2656.39, brown platelet, 0.58 × 0.31 × 0.17 mm, triclinic, *P* $\bar{1}$ EQ, *a* = 11.4781(3) Å, *b* = 14.4375(3) Å, *c* = 25.0402(18) Å, α = 93.474(7)°, β = 98.589(7)°, γ = 113.012(8)°, *U* = 3744.1(4) Å³, *Z* = 1, μ = 1.620 mm⁻¹, *F*(000) = 1398, *T* = 123(2)K. A total of 48 836 reflections were collected in the range 6.6° < 2θ < 62.4°. The 11 657 independent reflections [*R*(int) = 0.058] were used after absorption correction (*T*_{min} = 0.389, *T*_{max} = 1.000). Refinement of 812 parameters converged to *R*₁ = 0.0761 [for 8137 reflections having *I* > 2σ(*I*)], *wR*₂ = 0.2462 and goodness-of-fit of 1.10 (for all 11 657 *F*² data). Peak/hole 1.15/−0.88 e Å⁻³.

Crystal data for [ClO₄⊂(Cu₂L₂)](ClO₄)₃ (3). C₆₈H₉₂Cu₂N₈Cl₄O₂₄, *M_r* = 1674.38, green chunk, 0.24 × 0.16 × 0.16 mm, triclinic, *P* $\bar{1}$, *a* = 14.7464(8) Å, *b* = 15.6825(8) Å, *c* = 21.3265(15) Å, α = 95.308(7)°, β = 109.898(8)°, γ = 104.436(7)°, *U* = 4405.1(6) Å³, *Z* = 2, μ = 2.304 mm⁻¹, *F*(000) = 1748, *T* = 150(2)K. A total of 56 953 reflections were collected in the range 6.5° < 2θ < 61.2°. The 13 304 independent reflections [*R*(int) = 0.116] were used after absorption correction (*T*_{min} = 0.649, *T*_{max} = 1.000). Refinement of 1038 parameters converged to *R*₁ = 0.0828 [for 3644 reflections having *I* > 2σ(*I*)], *wR*₂ = 0.2413 and goodness-of-fit of 0.81 (for all 13 304 *F*² data). Peak/hole 0.45/−0.55 e Å⁻³.

Crystal data for [BF₄⊂(Cu₂L₂)](BF₄)₃·3C₃H₆O (4)·3C₃H₆O. C₆₈H₉₂Cu₂B₄F₁₂N₈O₈, 3(C₃H₆O), *M_r* = 1798.05, green platelet, 0.19 × 0.17 × 0.10 mm, triclinic, *P* $\bar{1}$, *a* = 11.7783(3) Å, *b* = 19.0859(5) Å, *c* = 20.9814(15) Å, α = 82.675(6)°, β = 77.892(5)°, γ = 75.638(5)°, *U* = 4453.4(4) Å³, *Z* = 2, μ = 1.383 mm⁻¹, *F*(000) = 1876,

$T = 123(2)\text{K}$. A total of 53 358 reflections were collected in the range $6.6^\circ < 2\theta < 61.2^\circ$. The 13 270 independent reflections [$R(\text{int}) = 0.075$] were used after absorption correction ($T_{\text{min}} = 0.452$, $T_{\text{max}} = 0.760$). Refinement of 1166 parameters converged to $R_1 = 0.0881$ [for 8153 reflections having $I > 2\sigma(I)$], $wR_2 = 0.2718$ and goodness-of-fit of 1.09 (for all 13 270 F^2 data). Peak/hole $0.92/-0.91 \text{ e } \text{\AA}^{-3}$.

Spectroscopic titrations

Spectrophotometric measurements in the UV-visible region were performed at 294 K using a CARY 100Bio UV-Vis spectrophotometer and 1 cm path length matched quartz cuvettes. Chemicals and solvents were of AR grade unless otherwise stated and used as received. The “metal only” complex **1** was dried *in vacuo* for two hours prior to the preparation of the titration solutions and the titrations were prepared immediately. Solutions of **1** in THF- CHCl_3 (CHCl_3 , less than 0.01%) (2 mL , $1.5 \times 10^{-5} \text{ mol L}^{-1}$) were titrated with THF solutions of the acid of interest ($2.5 \times 10^{-4} \text{ mol L}^{-1}$ – $1.0 \times 10^{-3} \text{ mol L}^{-1}$). Spectra were recorded following the addition of each aliquot over the wavelength range of 900 to 250 nm. The acid solutions were titrated at 0.25 molar equivalence increments for H_2SO_4 and 1.0 molar equivalence increments for HNO_3 , HClO_4 and HBr . A 1:1 anion to **1** binding model was assumed. Formation constants were calculated using the SPECFIT program (version 3.0.40, SPECFIT/32™).¹⁶ Titrations were repeated until three concordant results were obtained.

Notes and references

- 1 J. M. Holloway, R. A. Dahlgren, B. Hansen and W. H. Casey, *Nature*, 1998, **395**, 785–788; G. Hanrahan, M. Gledhill, P. J. Fletcher and P. J. Worsfold, *Anal. Chim. Acta*, 2001, **440**, 55–62; P. Chakrabarti, *J. Mol. Biol.*, 1993, **234**, 463–482; T. Yamaguchi, Y. Ikeda, Y. Abe, H. Kuma, D. Kang and N. Hamasaki, *J. Mol. Biol.*, 2010, **397**, 179–189; E. Pasqualetto, R. Aiello, L. Gesiot, G. Bonetto and M. Bellanda, *J. Mol. Biol.*, 2010, **400**, 448–462; K. Yoshizuka, H. Arita, Y. Baba and K. Inoue, *Hydrometallurgy*, 1990, **23**, 247–261; G. A. Kordosky, *Proc. Int. Solvent Extr. Conf.*, Cape Town, South Africa, 2002, pp. 853; B. Dietrich, *Pure Appl. Chem.*, 1993, **65**, 1457–1464.
- 2 P. A. Gale, *Coord. Chem. Rev.*, 2000, **199**, 181–233; L. A. J. Chrisstoffels, F. Jong, D. N. Reinhoudt, S. Sivelli, L. Gazzola, A. Casnati and R. Ungaro, *J. Am. Chem. Soc.*, 1999, **121**, 10142–10151.
- 3 J. M. Mahoney, K. A. Stucker, H. Jiang, I. Carmichael, N. R. Brinkmann, A. M. Beatty, B. C. Noll and B. D. Smith, *J. Am. Chem. Soc.*, 2005, **127**, 2922–2928; M. Cametti, M. Nissinen, A. D. Cort, L. Mandolini and K. Rissanen, *J. Am. Chem. Soc.*, 2005, **127**, 3831–3837; X. He and V. W. Yam, *Inorg. Chem.*, 2010, **49**, 2273–2279; M. Cametti, L. Ilander, A. Valkonen, M. Nieger, M. Nissinen, E. Nauha and K. Rissanen, *Inorg. Chem.*, 2010, **49**, 11473–11484; T. Riis-Johannessen, K. Schenk and K. Severin, *Inorg. Chem.*, 2010, **49**, 9546–9553; S. Shanmugaraju, A. K. Bar, K. Chi and P. S. Mukherjee, *Organometallics*, 2010, **29**, 2971–2980; Y. Xie and T. C. W. Mak, *J. Am. Chem. Soc.*, 2011, **133**, 3760–3763; A. M. J. Devoille, P. Richardson, N. L. Bill, J. L. Sessler and J. B. Love, *Inorg. Chem.*, 2011, **50**, 3116–3126; G. H. Clever, W. Kawamura and M. Shionoya, *Inorg. Chem.*, 2011, **50**, 4689.
- 4 P. G. Plieger, S. Parsons, A. Parkin and P. A. Tasker, *J. Chem. Soc., Dalton Trans.*, 2002, 3928–3930.
- 5 M. Wenzel, S. R. Bruere, Q. W. Knapp, P. A. Tasker and P. G. Plieger, *Dalton Trans.*, 2010, **39**, 2936–2941.
- 6 M. Wenzel, G. B. Jameson, L. A. Ferguson, Q. W. Knapp, R. S. Forgan, F. J. White, S. Parsons, P. A. Tasker and P. G. Plieger, *Chem. Commun.*, 2009, 3606–3608.
- 7 M. Wenzel, Q. W. Knapp and P. G. Plieger, *Chem. Commun.*, 2011, **47**, 499–501.
- 8 M. Wenzel, R. S. Forgan, A. Faure, K. Mason, P. A. Tasker, S. Piligkos, E. K. Brechin and P. G. Plieger, *Eur. J. Inorg. Chem.*, 2009, 4613–4617.
- 9 Q. Wang, C. Wilson, A. J. Blake, S. R. Collinson, P. A. Tasker and M. Schroder, *Tetrahedron Lett.*, 2006, **47**, 8983–8987.
- 10 T. J. Mooibroek, C. A. Black, P. Gamez and J. Reedijk, *Cryst. Growth Des.*, 2008, **8**, 1082–1093.
- 11 B. P. Hay and R. Custelcean, *Cryst. Growth Des.*, 2009, **9**, 2539–2545; L. A. Barrios, G. Aromi, A. Frontera, D. Quinero, P. M. Deya, P. Gamez, O. Roubeau, E. J. Shotton and S. J. Teat, *Inorg. Chem.*, 2008, **47**, 5873–5881.
- 12 Rigaku, *CrystalClear*, Version 1.4.0, Rigaku Americas Corporation, The Woodlands, Texas, USA, 2005.
- 13 Rigaku, *PROCESS-AUTO*, Rigaku Corporation, Tokyo, Japan, 1998.
- 14 G. M. Sheldrick, *Acta Crystallogr., Sect. A: Found. Crystallogr.*, 2008, **64**, 112–122.
- 15 P. Van der Sluis and A. L. Spek, *Acta Crystallogr., Sect. A: Found. Crystallogr.*, 1990, **46**, 194–201.
- 16 H. Gampp, M. Maeder, C. J. Meyer and A. D. Zuberbuehler, *Talanta*, 1985, **32**, 1133–1139; H. Gampp, M. Maeder, C. J. Meyer and A. D. Zuberbuehler, *Talanta*, 1985, **32**, 257–264; H. Gampp, M. Maeder, C. J. Meyer and A. D. Zuberbuehler, *Talanta*, 1985, **32**, 95–101.